

Model Studies of TTQ-Containing Amine Dehydrogenases

Shinobu Itoh,* Naoki Takada, Shigenobu Haranou, Takeya Ando, Mitsuo Komatsu, Yoshiki Ohshiro, and Shunichi Fukuzumi*

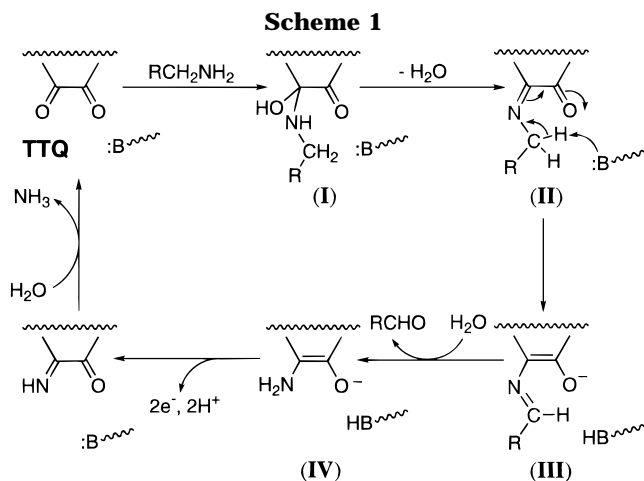
Department of Applied Chemistry, Faculty of Engineering, Osaka University, Yamada-oka 2-1, Suita, Osaka 565, Japan

Received September 4, 1996[®]

The reactions of a TTQ model compound [**1**, 3-methyl-4-(3'-methylindol-2'-yl)indole-6,7-dione] with several amines have been investigated in organic media to obtain mechanistic information on the action of quinoprotein methylamine and aromatic amine dehydrogenases. It has been found that compound **1** acts as an efficient catalyst for the autorecycling oxidation of benzylamine by molecular oxygen in CH₃OH. In order to evaluate the oxidation mechanism of amines by **1**, the product analyses and kinetic studies have been carried out under *anaerobic* conditions. In the first stage of the reaction of **1** with amines, **1** is converted into an iminoquinone-type adduct (so-called *substrate imine*), which was isolated and characterized by using cyclopropylamine as a substrate. The observed NOE of the isolated product indicates clearly that the addition position of the amine is C-6 of the quinone. The molecular orbital calculations suggest that the thermodynamic stability of the carbinolamine intermediate is a major factor to determine such regioselectivity; the C-6 carbinolamine is more stable than the C-7 counterpart by 2.9 kcal/mol. The reactivity of several primary amines and the electronic effect of the *p*-substituents of benzylamine derivatives in the iminoquinone formation suggest that the addition step of the amine to the quinone is rate-determining. When amines having an acidic α -proton such as benzylamine derivatives are employed as substrates, formation of the iminoquinone adduct was followed by rearrangement to the *product imine*. The kinetic analysis has revealed that this rearrangement consists of noncatalyzed and general base-catalyzed processes. Large kinetic isotope effects of 7.8 and 9.2 were observed for both the noncatalyzed and general base-catalyzed processes, respectively, since these steps involve a proton abstraction from the α -position of the substrate. In the reaction with benzhydrylamine, the product imine was isolated quantitatively and well characterized by several spectroscopic data. In the case of benzylamine, the product imine is further converted into the aminophenol derivative by the imine exchange reaction with excess benzylamine. These results indicate clearly that the amine oxidation by compound **1** proceeds via a *transamination* mechanism as suggested for the enzymatic oxidation of amines by TTQ cofactor.

Introduction

Bacterial methylamine dehydrogenase (MADH) and aromatic amine dehydrogenase (AADH) are the new class of enzymes that contain a novel heterocyclic *o*-quinone cofactor, TTQ (tryptophan tryptophylquinone), post-translationally derived from two tryptophan residues at the enzyme active site.^{1–3} Davidson and his co-workers have carried out detailed kinetic studies of the enzymatic redox reactions with several amines to propose the *transamination* mechanism for the enzymatic systems (Scheme 1).⁴ It is suggested that the reaction is initiated by a nucleophilic attack by the amine nitrogen on one of the quinone carbonyls, resulting in a carbinolamine



intermediate (I) that loses water to form an iminoquinone (II), the so-called *substrate imine*. An active-site base is proposed to abstract a proton from the α -carbon, causing rearrangement into *product imine* intermediate (III). Release of the aldehyde product then occurs by hydrolysis of the imine function of the intermediate (III) to produce aminophenol (IV) as a reduced cofactor. Incorporation of the substrate nitrogen into the reduced TTQ has been confirmed by ESR studies on the substrate-reduced MADH.^{4d} A similar mechanism has been proposed for quinoprotein amine oxidases that contain TPQ (2,4,5-trihydroxyphenylalanine quinone) as the redox cofactor.⁵

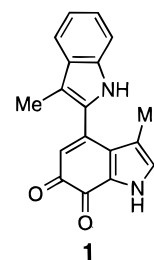
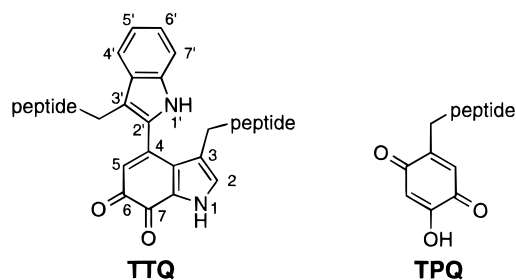
[®] Abstract published in *Advance ACS Abstracts*, November 15, 1996.

(1) McIntire, W. S.; Wemmer, D. E.; Chistoserdov, A.; Lidstrom, M. E. *Science* **1991**, *252*, 817.

(2) (a) Chen, L.; Mathews, F. S.; Davidson, V. L.; Huizinga, E. G.; Vellieux, F. M. D.; Duine, J. A.; Hol, W. G. J. *FEBS Lett.* **1991**, *287*, 163. (b) Chen, L.; Mathews, F. S.; Davidson, V. L.; Huizinga, E. G.; Vellieux, F. M. D.; Hol, W. G. J. *Proteins* **1992**, *14*, 288.

(3) Govindaraj, S.; Eisenstein, E.; Jones, L. H.; Sanders-Loehr, J.; Chistoserdov, A. Y.; Davidson, V. L.; Edwards, S. L. *J. Bacteriol.* **1994**, *176*, 2922.

(4) (a) Husain, M.; Davidson, V. L.; Gray, K. A.; Knaff, D. B. *Biochemistry* **1987**, *26*, 4139. (b) Davidson, V. L.; Jones, L. H.; Graichen, M. E. *Biochemistry* **1992**, *31*, 3385. (c) Brooks, H. B.; Jones, L. H.; Davidson, V. L. *Biochemistry* **1993**, *32*, 2725. (d) Warncke, K.; Brooks, H. B.; Babcock, G. T.; Davidson, V. L.; McCracken, J. J. *Am. Chem. Soc.* **1993**, *115*, 6464. (e) Hyun, Y.-L.; Davidson, V. L. *Biochemistry* **1995**, *34*, 816. (f) Davidson, V. L.; Graichen, M. E.; Jones, L. H. *Biochem. J.* **1995**, *308*, 487.



Experimental Section

Environmental effects at the enzyme active site, however, often obscure the kinetic data. For example, the rate constant for the α -proton abstraction step (II to III in Scheme 1) of phenethylamine in AADH is 2-orders of magnitude larger than that of benzylamine,^{4e} and the rate constant for methylamine is larger than that of benzylamine by 10^4 -fold in MADH.^{4b,c} Judging from the acidity of the α -proton of those substrates, such results may indicate that the location of the α -proton of the artificial substrate (benzylamine) is forced to move away from the suitable place for the general base catalysis by steric restriction in the enzyme active site. Observation of the large deuterium kinetic isotope effect (17.2 for methylamine in MADH)^{4c} indicates that the α -proton abstraction is the rate-determining step. With regard to the addition position of the amine to the quinone, it has been shown to be C-6 by the result of X-ray crystallographic analysis of the hydrazine-derivatized enzyme, where the 6-position of TTPQ is modified selectively.⁶ It is believed that the major factor controlling the addition position of the substrate is the three-dimensional structure at the enzyme active site, in which there is enough space for substrate-binding only near the C-6 carbonyl group.^{2a} In order to assess such environmental factors at the enzyme active site, it is essential to know the direct reactivity of TTPQ itself toward amines. Cofactor TTPQ is, however, formed by post-translational modification of the two tryptophan side chains and thereby tightly associated in the enzyme matrix, making it very difficult to isolate the cofactor intact.⁷

Recently, we have developed a synthetic model (**1**) of TTPQ cofactor that shows the molecular geometry, redox potential, and several spectroscopic characteristics, similar to those of the native enzymes, indicating that compound **1** is a very good *structural model* for MADH and AADH.⁸ In this paper we would like to report the first model studies on the action of TTPQ-containing amine dehydrogenases.⁹ The present study provides valuable insight into the amine oxidation mechanism by TTPQ as well as the chemistry of the newly found quinone cofactors.^{10–12}

The model compound (**1**) was obtained from the previous study.⁸ α,α -Dideuteriobenzylamine was prepared by the reduction of benzamide with LiAlD₄ in THF according to the general procedure, and its purity (>99%) was determined by ¹H NMR and MS. All other chemicals used in this study were commercial products of the highest available purity and were further purified by standard methods, if necessary.¹³ Melting points are uncorrected. Mass spectra were determined at an ionization voltage of 70 eV. ¹H NMR and ¹³C NMR spectra were recorded at 270 MHz using CDCl₃ or DMSO-*d*₆ as a solvent and TMS as an internal reference. The cyclic voltammetry measurements were performed with a three-electrode system consisting of a glassy carbon working electrode, a platinum plate auxiliary electrode, and an SCE reference electrode. The glassy carbon electrode was polished with 0.05-mm alumina powder, sonicated to remove the powder, and washed with water. All electrochemical measurements were carried out at 25 °C under an atmospheric pressure of nitrogen.

Molecular orbital calculations were performed with the MOPAC program (Version 6) by using a CAChe Work System (SONY Tektronix) and a MOL-GRAFF program (Version 2.8 supplied by Daikin Industries, Ltd.).¹⁴ Final geometries and energetics were obtained by optimizing the total molecular energy with respect to all structural variables.

Catalytic Oxidation of Benzylamine under O₂. The catalytic oxidation of benzylamine with molecular oxygen was initiated by adding the amine (1.0 mmol), with a microsyringe, to an O₂-saturated CH₃OH solution (10 mL) of **1** (1 mM), when the initial amine concentration was 100 mM. The mixture was stirred at room temperature under O₂ atmosphere. The rate of formation of benzaldehyde was monitored by HPLC [pump: Hitachi L-600; UV-detector: Hitachi 638–0430 UV monitor; column: Waters radial compression separation system (C₁₈); eluent: CH₃OH/H₂O/H₃PO₄, 45:54.5:0.5]. The ¹H NMR and IR spectra of the concentrated final reaction mixture indicated that *N*-benzylidenebenzylamine (PhCH₂N=CHPh) was formed quantitatively: ¹H NMR (CDCl₃) δ 4.80 (2 H, s, –CH₂–), 7.20–7.50 (8 H, m, aromatic protons), 7.70–7.85 (2 H, m, aromatic protons), 8.38 (1 H, br s, –CH=); IR (neat) 1648 cm^{–1} (C=N).

Kinetic Analysis. The reactions of **1** and several amines were followed by the UV–vis spectra under the pseudo-first-order conditions with excess amine in deaerated CH₃OH at 30 °C. Typically, a CH₃OH solution of **1** (5.0×10^{-5} M) was placed in a UV cell (1 cm path length, sealed tightly with a silicon rubber cap) and was deaerated by bubbling Ar through it for ca. 20 min. Then the amine was added with a microsyringe to start the reaction. The pseudo-first-order rate constant (*k*_{obs}) was calculated from the rate of a decrease in the intensity of the absorption due to **1** (420 nm) or an increase in the intensity of the absorption due to the products. The nonlinear curve-fitting program (Mac curve fit) was used to

(5) (a) Janes, S. M.; Mu, D.; Wemmer, D.; Smith, A. J.; Kaur, S.; Maltby, D.; Burlingame, A. L.; Klinman, J. P. *Science* **1990**, *248*, 981. (b) Jones, S. M.; Klinman, J. P. *Biochemistry* **1991**, *30*, 4599. (c) Hartmann, C.; Klinman, J. P. *Biochemistry* **1991**, *30*, 4604. (d) Hartmann, C.; Brzovic, P.; Klinman, J. P. *Biochemistry* **1993**, *32*, 2234. (6) Huizinga, E. G.; van Zanten, B. A. M.; Duine, J. A.; Jongejan, J. A.; Huitema, F.; Wilson, K. S.; Hol, W. G. J. *Biochemistry* **1992**, *31*, 9789.

(7) Chistoserdov, A. Y.; Tsygankov, Y. D.; Lidstrom, M. E. *Biochem. Biophys. Res. Commun.* **1990**, *172*, 211.

(8) (a) Itoh, S.; Ogino, M.; Komatsu, M.; Ohshiro, Y. *J. Am. Chem. Soc.* **1992**, *114*, 7294. (b) Itoh, S.; Ogino, M.; Haranou, S.; Terasaka, T.; Ando, T.; Komatsu, M.; Ohshiro, Y.; Fukuzumi, S.; Kano, K.; Takagi, K.; Ikeda, T. *J. Am. Chem. Soc.* **1995**, *117*, 1485.

(9) Preliminary results have been published: Ohshiro, Y.; Itoh, S. *Pure Appl. Chem.* **1994**, *66*, 753.

(10) Itoh, S.; Ogino, M.; Fukui, Y.; Murao, H.; Komatsu, M.; Ohshiro, Y.; Inoue, T.; Kai, Y.; Kasai, N. *J. Am. Chem. Soc.* **1993**, *115*, 9960.

(11) (a) Mure, M.; Klinman, J. P. *J. Am. Chem. Soc.* **1993**, *115*, 7117. (b) Mure, M.; Klinman, J. P. *J. Am. Chem. Soc.* **1995**, *117*, 8698. (c) Mure, M.; Klinman, J. P. *J. Am. Chem. Soc.* **1995**, *117*, 8707.

(12) (a) Wang, F.; Base, J.-Y.; Jacobson, A. R.; Lee, Y.; Sayre, L. M. *J. Org. Chem.* **1994**, *59*, 2409. (b) Lee, Y.; Sayre, L. M. *J. Am. Chem. Soc.* **1995**, *117*, 3096. (c) Lee, Y.; Sayre, L. M. *J. Am. Chem. Soc.* **1995**, *117*, 11823.

(13) Perrin, D. D.; Armarego, W. L. F.; Perrin, D. R., *Purification of Laboratory Chemicals*; Pergamon Press: Elmsford, NY, 1966.

(14) The PM3 method: Stewart, J. J. P. *J. Comput. Chem.* **1989**, *10*, 209, 221.

determine the rate constants in case the final value of the absorbance (A_{∞}) was obscured by the followup reaction.

Product Analysis. Reaction with Cyclopropylamine. A CH_3CN solution of **1** (2.0 mM) was placed in a reaction vessel that was sealed tightly with a silicon rubber cap and was deaerated by bubbling Ar through it for ca. 20 min. Then cyclopropylamine (10 equiv) was introduced with a microsyringe into the solution, and the reaction mixture was stirred at 25 °C for 4 h under dark. Removal of the solvent and the excess amine under reduced pressure gave iminoquinone **3** as an orange solid quantitatively. Iminoquinone **3** exists as a mixture of syn-anti-type stereoisomers at the imine function at C-6 (major:minor = 5:1): mp > 300 °C; IR (KBr) 3290 (NH), 1632 cm^{-1} (C=O and C=N); UV-vis (CH_3CN) λ_{max} 227 nm ($\epsilon = 3.9 \times 10^4 \text{ M}^{-1} \text{ cm}^{-1}$), 280 (2.0×10^4), 390 (1.1×10^4); ^1H NMR (270 MHz, $\text{DMSO}-d_6$) major isomer **3a** δ 1.08–1.40 (4 H, m, cyclopropyl $-\text{CH}_2\text{CH}_2-$), 1.50 (3 H, s, CH_3 -3), 2.26 (3 H, s, CH_3 -3'), 5% NOE was detected when irradiated at H-5), 3.68 (1 H, m, cyclopropyl $-\text{CH}-$, 20% NOE was detected when irradiated at H-5), 6.66 (1 H, s, H-5), 6.97–7.14 (3 H, m, H-2, H-5', and H-6'), 7.32 (1 H, d, $J = 7.3 \text{ Hz}$, H-7'), 7.52 (1 H, d, $J = 7.3 \text{ Hz}$, H-4'), 11.14 (1 H, br s, H-1'), 12.33 (1 H, br s, H-1'); minor isomer **3b** 2.22 (3 H, s, CH_3 -3'), 5.56 (1 H, m, cyclopropyl $-\text{CH}-$), 6.04 (1 H, s, H-5), 7.31 (1 H, d, $J = 7.3 \text{ Hz}$, H-7'), 7.51 (1 H, d, $J = 7.3 \text{ Hz}$, H-4'), 11.09 (1 H, br s, H-1'), other protons of the minor product were overlapped with those of the major isomer; ^{13}C NMR ($\text{DMSO}-d_6$) for the major isomer 9.1 ($-\text{CH}_3$), 9.9 ($-\text{CH}_3$), 13.7, 30.7, 36.9 (cyclopropyl carbon), 107.9, 111.1, 114.7, 118.1, 118.5, 118.6, 121.6, 127.7, 128.0, 128.3, 131.8, 132.2, 135.5, 135.7 (14 aromatic carbons), 156.9 (6-C), 171.0 (7-C) ppm; high resolution MS m/e 329.1526 (M^+) calcd for $\text{C}_{21}\text{H}_{19}\text{ON}_3$ 329.152 97.

Reduction of the mixture by methylhydrazine (30 equiv) in deaerated CH_3CN gave **5** as a brown solid quantitatively: mp > 300 °C; IR (KBr) 3420 cm^{-1} (OH and NH); ^1H NMR (270 MHz, $\text{DMSO}-d_6$) δ 1.20–1.23 (4 H, m, cyclopropyl $-\text{CH}_2\text{CH}_2-$), 1.41 (3 H, s, CH_3 -3), 2.22 (3 H, s, CH_3 -3'), 3.69 (1 H, m, cyclopropyl $-\text{CH}-$), 5.89 (1 H, s, H-5), 6.96–7.06 (3 H, m, H-2, H-5', and H-6'), 7.29 (1 H, d, $J = 7.8 \text{ Hz}$, H-7'), 7.48 (1 H, d, $J = 7.8 \text{ Hz}$, H-4'), 10.20 (1 H, br s, NH), 11.00 (1 H, br s, H-1'), 11.99 (1 H, br s, H-1'); MS EI m/e 331 (M^+).

Reaction with Benzhydrylamine. The reaction of **1** and benzhydrylamine (20 equiv) was carried out in a similar manner for 2 h. Removal of the solvent gave a brown residue from which **8** was obtained as a yellow powder in 98% yield by recrystallization with ether and *n*-hexane: mp 97–99 °C; IR (KBr) 3440 (OH), 3080 (NH), 1603 cm^{-1} (C=N); UV-vis (CH_3CN) λ_{max} 405 nm ($\epsilon = 5.0 \times 10^3 \text{ M}^{-1} \text{ cm}^{-1}$); ^1H NMR (270 MHz, $\text{DMSO}-d_6$) δ 1.62 (3 H, s, CH_3 -3), 1.68 (3 H, s, CH_3 -3'), 5.6% NOE was detected when irradiated at H-5), 5.99 (1 H, s, H-5), 6.88–7.01 (2 H, m, aromatic proton), 7.14–7.51 (12 H, m, aromatic proton, totally 27% NOE was detected when irradiated at H-5), 7.71 (1 H, d, $J = 7.3 \text{ Hz}$, H-4'), 8.85, 10.67, 10.76 (each 1 H, br s, NH $\times 2$ and OH); ^{13}C NMR ($\text{DMSO}-d_6$) 8.7 (CH_3), 10.7 (CH_3), 106.4, 110.5, 115.2, 116.1, 117.8, 120.2, 123.3, 125.2, 126.4, 126.7, 128.1, 128.3, 128.4, 128.7, 128.9, 130.0, 130.4, 134.8, 134.9, 137.2, 139.8 (aromatic carbons), 166.7 (C=N) ppm; high resolution MS m/e 455.2014 (M^+) calcd for $\text{C}_{31}\text{H}_{25}\text{ON}_3$ 455.199 95.

Reaction with Benzylamine. The reaction of **1** with benzylamine (10 equiv) was carried out similarly in CH_3OH for 3 h under anaerobic conditions. The precipitated dark violet solid was collected by centrifugation, washed with ether, and dried under vacuo to obtain aminophenol **12** quantitatively: mp > 300 °C; IR (KBr) 3432 cm^{-1} (NH); UV-vis (CH_3CN containing 2% DMSO) λ_{max} 326 nm ($\epsilon = 7.0 \times 10^3 \text{ M}^{-1} \text{ cm}^{-1}$), 511 (3.6×10^3), and 771 (5.5×10^3); ^1H NMR (270 MHz, $\text{DMSO}-d_6$) δ 1.70 (3 H, s, CH_3 -3), 2.27 (3 H, s, CH_3 -3'), 3.6 (3 H, br s, OH and NH_2), 7.00–7.14 (4 H, m, H-2, H-5, H-5', and H-6'), 7.30 (1 H, d, $J = 8.1 \text{ Hz}$, H-4' or H-7'), 7.49 (1 H, d, $J = 8.1 \text{ Hz}$, H-4' or H-7'), 11.12 (1 H, br s, NH), 12.23 (1 H, br s, NH); ^{13}C NMR ($\text{DMSO}-d_6$) 9.6 (CH_3), 11.02 (CH_3), 108.8, 111.2, 113.6, 117.5, 118.8, 122.0, 126.4, 127.4, 128.1, 128.3, 128.7, 133.2, 136.0, 165.4 (aromatic carbons) ppm; MS EI, pos, m/e 291 (M^+).

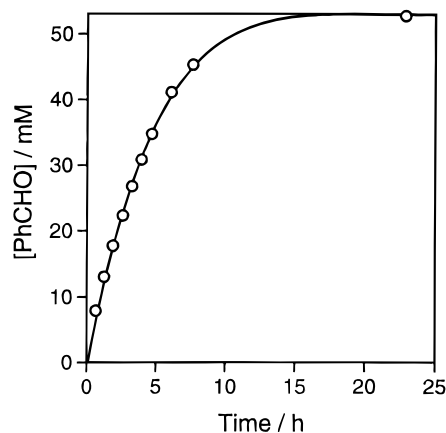
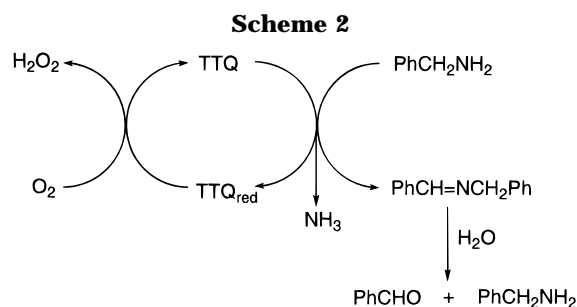


Figure 1. Time course of the oxidation of benzylamine (100 mM) catalyzed by **1** (1.0 mM) in CH_3OH solution under aerobic conditions. The formation of benzaldehyde was monitored by HPLC (see Experimental Section).



From the supernatant, *N*-benzylidenebenzylamine ($\text{PhCH}_2\text{N}=\text{CHPh}$) was obtained quantitatively.

Results and Discussion

Catalytic Oxidation of Benzylamine by **1 under O_2 .** MADH and AADH catalyzed oxidative deamination of primary amines to the corresponding aldehydes as illustrated in Scheme 1. The two electrons obtained from the amine substrates were transferred to an electron acceptor enzyme such as Amicyanin.¹⁵ In vitro, phenazine ethosulfate (PES) can be used as an electron acceptor for the steady-state kinetic analysis of the enzymatic reactions.¹⁶ In our model system, the catalytic activity of **1** in the amine oxidation was examined by using O_2 as the electron acceptor (so-called aerobic autorecycling system). It was found that treatment of benzylamine (100 mM) with a catalytic amount (1 mol %) of **1** in CH_3OH under O_2 atmosphere gave *N*-benzylidenebenzylamine ($\text{PhCH}_2\text{N}=\text{CHPh}$), which was isolated quantitatively (see the Experimental Section). Thus, our TTQ model compound (**1**) acts as an efficient catalyst in the oxidation of benzylamine by O_2 (Scheme 2). Figure 1 shows the time course of the catalytic reaction that was monitored by following the formation of benzaldehyde by HPLC. The maximum amount of benzaldehyde formed is 50 mM, since $\text{PhCH}_2\text{N}=\text{CHPh}$ is spontaneously converted into PhCHO and PhCH_2NH_2 by hydrolysis in the HPLC column (Scheme 2).

(15) (a) Gray, K. A.; Davidson, V. L.; Knaff, D. B. *J. Biol. Chem.* **1988**, *263*, 13987. (b) Kumar, M. A.; Davidson, V. L. *Biochemistry* **1990**, *29*, 5299. (c) Chen, L.; Durley, R.; Poliks, B. J.; Hamada, K.; Chen, Z.; Mathews, F. S.; Davidson, V. L.; Satow, Y.; Huizinga, E.; Vellieux, F. M. D.; Hol, W. G. J. *Biochemistry* **1992**, *31*, 4959. (d) Chen, L.; Durley, R. C. E.; Mathews, F. S.; Davidson, V. L. *Science* **1994**, *264*, 86. (e) Brooks, H. B.; Davidson, V. L. *Biochemistry* **1994**, *33*, 5696. (f) Brooks, H. B.; Davidson, V. L. *J. Am. Chem. Soc.* **1994**, *116*, 11201. (16) Davidson, V. L. *Biochem. J.* **1989**, *261*, 107.

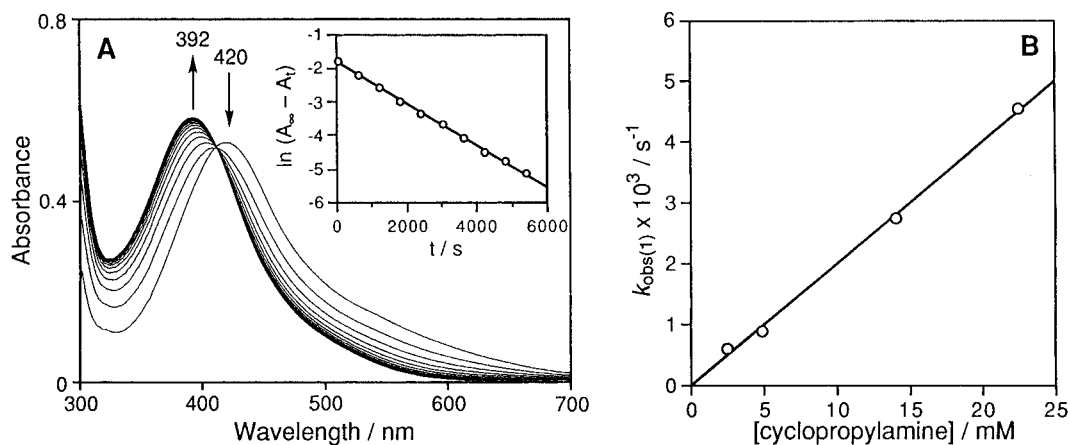


Figure 2. (A) Spectral change observed upon addition of cyclopropylamine (2.5×10^{-3} M) to the methanol solution of **1** (5.0×10^{-5} M) at 30°C under anaerobic conditions; interval, 600 s. Inset: The pseudo-first-order plot. (B) Dependence of k_{obs} on the cyclopropylamine concentration.

Table 1. Aerobic Oxidation of Benzylamine Catalyzed by Quinones in CH_3OH ^a

quinone	$E_{1/2}^b$	yield (%) of PhCHO ^c
9,10-phenanthrenequinone	-232	50
1	-188	3700
1,2-naphthoquinone	-186	0
1,7-phenanthrolinequinone	-102	1600
3,5-di- <i>tert</i> -butyl-1,2-benzoquinone	33	600
1,4-benzoquinone	79	0

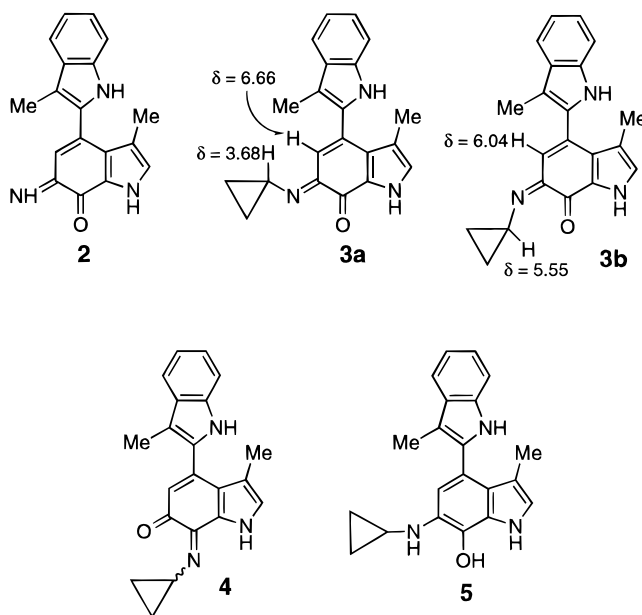
^a [Quinone] = 1.0 mM, [PhCH₂NH₂] = 100 mM, under O₂, in CH₃OH. ^b Two-electron redox potential vs SCE determined by cyclic voltammetry in 0.1 M phosphate buffer containing 30% CH₃CN (pH 7.3). ^c Yield of PhCHO in 5 h determined by HPLC based on the quinone.

The catalytic efficiency of **1** was compared to that of ordinary quinone compounds. The product yields in 5 h (earlier stage of the reaction) based on the amount of quinones are listed in Table 1 together with their two-electron redox potentials (vs SCE) measured in aqueous media. 1,7-Phenanthrolinequinone also acts as a catalyst, but its catalytic efficiency is lower than **1**. On the other hand, 3,5-di-*tert*-butyl-1,2-benzoquinone, a well-known reagent for amine oxidation (Corey's reagent), is a poor catalyst and other ordinary *o*- and *p*-quinones do not work at all in this system. It is interesting to note that there is no correlation between the catalytic efficiency and the redox potentials of those quinones. For example, the catalytic activities of compound **1** and 1,2-naphthoquinone are completely different, although they have essentially the same redox potentials. These results indicate that a simple electron-transfer mechanism may not be involved in the amine oxidation process.¹⁷

Formation of Iminoquinone (Substrate Imine).

We have previously demonstrated that compound **1** is easily transformed into iminoquinone **2** in the reaction with NH₃.^{8b} Similarly, an iminoquinone-type adduct **3** was obtained quantitatively in the reaction with cyclopropylamine. The ¹H NMR spectrum of the product indicates that there are two isomers in a ca. 5:1 ratio (see the Experimental Section). The major product **3a** shows a large NOE (20%) between H-5 and H- α (the methyne proton of the cyclopropyl ring, δ 3.68), which indicates that the addition position of the amine in the

major product is C-6. A possibility of the minor product being a C-7 regioisomer **4** can be ruled out by the result that reduction of the product mixture by methylhydrazine gave only one isomer of the reduced product **5** (see the Experimental Section). If the minor product was the C-7 regioisomer, the reduction would also provide two C-6 and C-7 regioisomers of the aminophenol products. Thus, it can be concluded that the minor product **3b** is a syn-anti-type stereoisomer at the imine function at C-6. In the ¹H NMR, H-5 of **3a** (δ = 6.66) and H- α of **3b** (5.55) appear at relatively low magnetic field as compared to the normal peaks, H-5 of **3b** (6.04) and H- α of **3a** (3.68), respectively. Such downfield shifts can be realized by considering the magnetic anisotropy effect of the cyclopropyl ring for H-5 in **3a** and that of the C-7 carbonyl group for H- α in **3b**, respectively.¹⁸



The iminoquinone formation in the reaction of **1** with cyclopropylamine was followed by monitoring the UV-vis spectrum in CH₃OH as shown in Figure 2A. A remarkable increase in the absorption at 392 nm due to the iminoquinone accompanied by a decrease at 420 nm

(17) The oxidation of the reduced species of compound **1** by O₂ is much faster than the reaction of **1** with amines under the reaction conditions employed.

(18) Rahman, A. *Nuclear Magnetic Resonance*; Springer-Verlag: New York, 1986.

Table 2. Second-Order Rate Constants (k_1) for the Iminoquinone Formation and λ_{\max} of the Products^a

amine	λ_{\max}/nm	$k_1/\text{M}^{-1} \text{s}^{-1}$
<i>n</i> -propylamine	402	1.37
benzylamine	400	0.27
cyclopropylamine	392	0.20
cyclohexylamine	391	0.16
isopropylamine	392	0.12
benzhydrylamine	405	0.0087
<i>tert</i> -butylamine	NR ^b	

^a [Quinone] = 5.0×10^{-5} M, in CH₃OH, at 30 °C, under N₂.
^b No reaction.

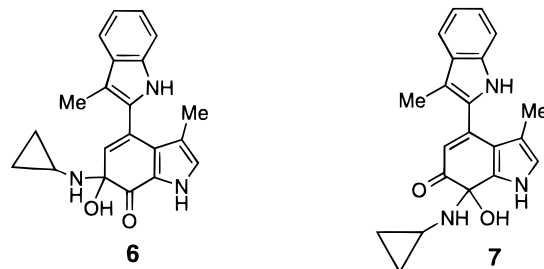
due to the quinone itself is observed with a clear isosbestic point at 412 nm. Observation of such a clear isosbestic point at 412 nm suggests that the syn-anti-type stereoisomers (**3a** and **3b**) have the same absorption spectra. The increase in the absorbance at 392 nm obeys the pseudo-first-order rate law (inset of Figure 2A), from which the pseudo-first-order rate constant $k_{\text{obs}(1)}$ was obtained. The plot of $k_{\text{obs}(1)}$ vs the cyclopropylamine concentration (0–25 mM) gave a straight line passing through the origin without any saturation phenomenon (Figure 2B), suggesting that the addition step of the amine to the quinone carbonyl group is rate-determining in the iminoquinone formation process under the experimental conditions. A similar spectral change (iminoquinone formation) was observed in the case of other primary alkylamines such as *n*-propylamine, isopropylamine, and cyclohexylamine. The second-order rate constants k_1 , obtained from the slope of the linear plot of $k_{\text{obs}(1)}$ vs the amine concentration, are listed in Table 2 together with λ_{\max} of the iminoquinone products (for benzylamine and benzhydrylamine, *vide infra*). The order of the reactivity of the amines in the addition reaction reflects clearly the steric bulkiness around the amino group of the substrates; the (primary alkyl)amine reacts more readily than the (secondary alkyl)amines, and the (tertiary alkyl)amine gives no appreciable amount of the iminoquinone product. Since the iminoquinones derived from these alkylamines are relatively stable under the experimental conditions, they are poor substrates in the aerobic amine oxidation reaction.¹⁹

Regioselectivity in Formation of the Amine Adduct. In the enzymatic system, the addition position of the amine to TTQ cofactor has been shown to be the C-6 quinone carbonyl carbon.^{2a} Steric restriction at the enzyme active site is believed to be the major factor causing such a regioselectivity as mentioned above. However, we have shown that the primary amines form the C-6 iminoquinone adducts selectively with **1** without the enzyme. Thus, the regioselectivity in the adduct formation may be ascribed to a chemical characteristic of the TTQ cofactor itself as well.

In order to evaluate the origin of the regioselectivity in the adduct formation, we performed semiempirical molecular orbital calculations on **1** and its cyclopropylamine adducts using the MOPAC program (PM3 method). Both the eigenvalues of LUMO and the net atomic charge at C-7 are larger than those at C-6 (eigenvalues of LUMO, C-6: 0.327, C-7: 0.335; atomic charge, C-6: 0.276, C-7: 0.322), suggesting that the addition position of the amine is not controlled by the electronic structure

(19) In contrast to benzylamine, other amines (*n*-propylamine, isopropylamine, cyclopropylamine, cyclohexylamine, and benzhydrylamine) do not undergo any significant deamination: the yields of the carbonyl products were 0–120% on the basis of **1** in 24 h under the same experimental conditions.

of the quinone. On the other hand, the heat of formation (ΔH_f) of C-6 carbinolamine **6** is lower than that of the C-7 adduct **7** by 2.9 kcal/mol (13.9 kcal/mol and 16.8 kcal/mol, respectively), while the C-6 iminoquinone **3a** and the C-7 iminoquinone **4** have the same ΔH_f values (75.7 kcal/mol). Thus, the difference in the thermodynamic stability of the carbinolamine intermediate may be the major factor to determine the regioselectivity in the adduct formation.



Formation of Product Imine. When benzhydrylamine is used as a substrate, the reaction continues from the iminoquinone stage to give the product imine **8**, which was isolated from a preparative-scale reaction with **1** in CH₃OH (see Experimental Section). The large NOE (27%) detected between H-5 and phenyl protons of the amine moiety indicates that the addition position of the amine is also C-6 and the direction of the imine function is *trans* against the C(6)–C(7) double bond as illustrated below. The decreasing NOE between H-5 and Me-3 (5.6%) compared to that observed in **1** (20%)⁸ would suggest that the dihedral angle of the two indole rings in **8** increases as compared to **1** (46.9°)⁸ because of the increasing steric repulsion between the phenyl ring and Me-3'.²⁰ The upfield shifts of Me-3' ($\delta = 1.68$, *cf.* $\delta = 2.31$ in **1**, 2.27 in **2**, 2.26 in **3a**) could be attributed to the magnetic anisotropy effect by the phenyl ring of the amine moiety. All these results can be explained when the addition position of the amine is C-6. The product imine **8** is very stable, and no further reaction occurred to afford the aminophenol derivative because the imine function is conjugated with both the two phenyl rings and the indole ring. This is the reason why benzhydrylamine is not a good substrate for the catalytic reaction by **1**.¹⁹

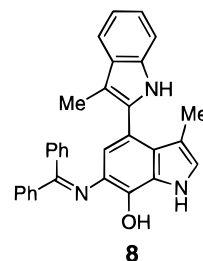


Figure 3A shows the spectral change of the reaction of **1** with benzhydrylamine, where the initial spectral change shows no isosbestic point, but at the prolonged reaction time, a clear isosbestic point is observed at 355 nm. Such a spectral change in Figure 3A may be attributed to the formation of the iminoquinone at the initial stage as observed in the reaction of **1** and cyclopropylamine (Figure 2A) and the subsequent formation

(20) The molecular orbital calculation suggested that the reduction of the quinone moiety itself also causes the increase of the dihedral angle between the two indole rings. The calculated value of the dihedral angle is ca. 58.5° in the quinol form (TTQH₂).

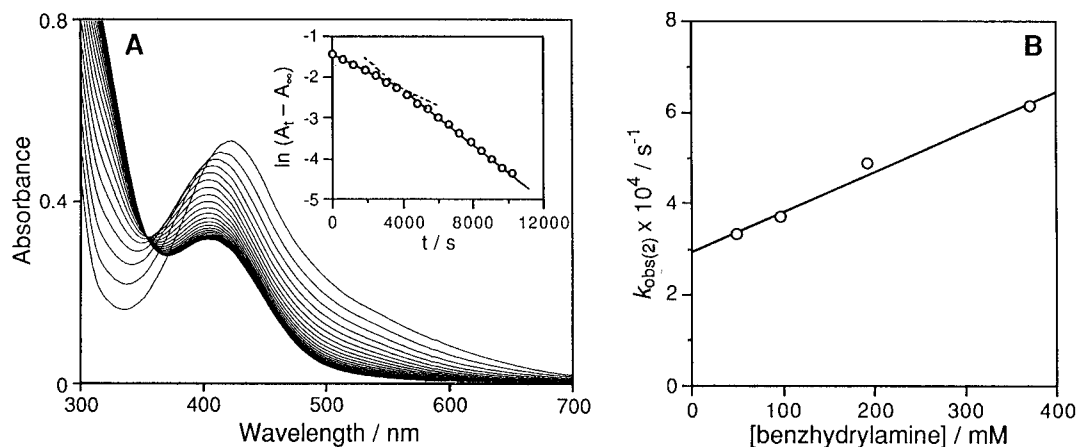
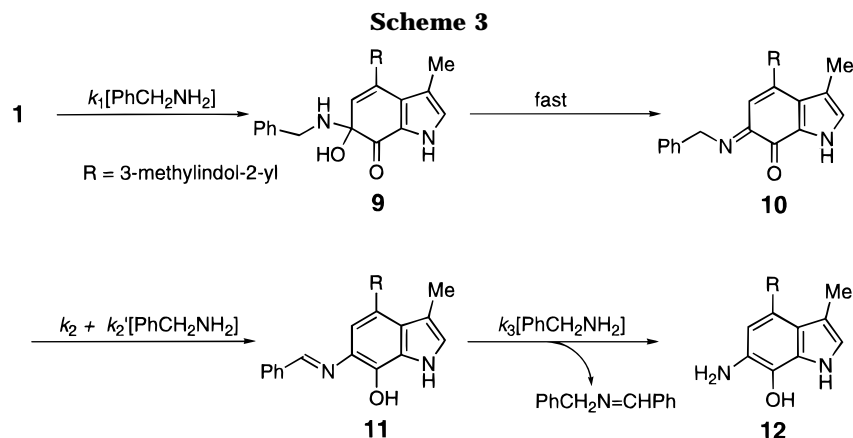


Figure 3. (A) Spectral change observed upon addition of benzhydrylamine (5.0×10^{-2} M) to the methanol solution of **1** (5.0×10^{-5} M) at 30 °C under anaerobic conditions; interval, 600 s. Inset: Plot of $\ln(A_t - A_\infty)$ vs time at 420 nm. (B) Dependence of k_{obs} on the benzhydrylamine concentration.



of the product imine ($\lambda_{\text{max}} = 405$ nm) from the iminoquinone intermediate. Thus, the plot of $\ln(A_t - A_\infty)$ at 420 nm vs time exhibits the biphasic behavior as shown in the inset of Figure 3A. The kinetics consisting of two consecutive steps was analyzed with two exponential terms by using a computer simulation (see Experimental Section). The pseudo-first-order rate constant $k_{\text{obs}(1)}$ for the initial iminoquinone formation thus determined was proportional to the amine concentration. The second-order rate constant k_1 for the iminoquinone formation is determined as $8.7 \times 10^{-3} \text{ M}^{-1} \text{ s}^{-1}$ from the linear plot of $k_{\text{obs}(1)}$ vs [amine]. The small k_1 value of benzhydrylamine as compared to those of other alkylamines (Table 2) may be attributed to the bulkiness around the amino group due to the two phenyl rings. Dependence of the pseudo-first-order rate constant $k_{\text{obs}(2)}$ of the second step on the amine concentration is shown in Figure 3B, in which there is an intercept at [amine] = 0. This can be expressed by eq 1, where k_2 is the rate constant for the

$$k_{\text{obs}(2)} = k_2 + k_2'[\text{amine}] \quad (1)$$

spontaneous rearrangement from the corresponding iminoquinone to product imine **8** and k_2' is for the general base-catalyzed rearrangement. In the latter case, the substrate amine acts as the general base catalyst as well. From the linear plot in Figure 3B, k_2 and k_2' are determined as $2.9 \times 10^{-4} \text{ s}^{-1}$ and $8.9 \times 10^{-4} \text{ M}^{-1} \text{ s}^{-1}$, respectively.

Mechanism of Benzylamine Oxidation. When benzhydrylamine is replaced by benzylamine in the

reaction with **1**, the final product was isolated as aminophenol **12** quantitatively (see Experimental Section).²¹ The aminophenol product may be produced by the further reaction of the product imine intermediate **11** that was formed from iminoquinone **10** as shown in Scheme 3.

In order to confirm the reaction mechanism in Scheme 3, the reaction of **1** with benzylamine was further investigated in CH_3OH . At low concentrations of benzylamine (below 1.5 mM), the iminoquinone formation is observed predominantly as shown in Figure 4, which is similar to that observed in the case of simple alkylamines (Figure 2). The k_1 value for the iminoquinone formation was determined as $0.27 \text{ M}^{-1} \text{ s}^{-1}$ from the slope of the linear plot of $k_{\text{obs}(1)}$ vs [amine] as shown in the inset of Figure 4. The k_1 values of benzylamine derivatives having several *p*-substituents ($-\text{X}$) were also determined in a similar manner, and they are listed in Table 3. The difference of the k_1 values for the iminoquinone formation is not so large, but there is a good correlation between $\log k_{1X}$ vs δ_p as shown in Figure 5 ($\rho = -0.26$, $r^2 = 0.989$).

(21) It should be mentioned that the isolated product has very broad absorptions at 511 and 771 nm that also exist in the final spectrum (b) shown in Figure 6. We assume that such characteristic absorptions at the visible region of the product are due to the formation of a charge-transfer-type molecular aggregation since the monomeric reduced form of **1** would not have such broad visible absorptions.⁸ The catalytic oxidation of benzylamine also occurs when the isolated product **12** is treated with an excess amount of benzylamine under O_2 atmosphere in CH_3OH . This result clearly indicates that the oxidation-active quinone form is regenerated from the isolated product by O_2 , indicating that it is actually an oxygen-sensitive aminophenol derivative as expected.

(22) Hansch, C.; Leo, A.; Taft, R. W. *Chem. Rev.* **1991**, *91*, 165.

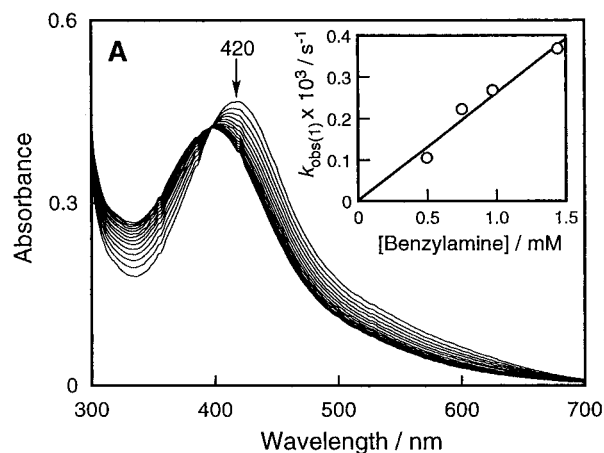


Figure 4. Spectral change observed upon addition of benzylamine (1.0×10^{-3} M) to the methanol solution of **1** (5.0×10^{-5} M) at 30°C under anaerobic conditions; interval, 600 s. Inset: Dependence of k_{obs} on the benzylamine concentration.

Table 3. Rate Constants k_1 and k_2 in the Reactions of **1** with *p*-Substituted Benzylamines (*p*-XC₆H₄CH₂NH₂)^a

-X	δ_p^b	$k_1/\text{M}^{-1}\text{s}^{-1}$	$k_{\text{obs}(2)}/\text{s}^{-1}$
OCH ₃	-0.27	0.33	2.3×10^{-3}
CH ₃	-0.17	0.29	2.7×10^{-3}
H	0	0.27	2.3×10^{-3}
F	0.06	0.25	1.7×10^{-3}
Cl	0.23	0.23	1.5×10^{-3}
NO ₂	0.78	0.17	4.2×10^{-4}

^a [Quinone] = 5.0×10^{-5} M, in CH₃OH, at 30°C , under N₂.
^b Taken from ref 22. ^c At [amine] = 2.0×10^{-2} M.

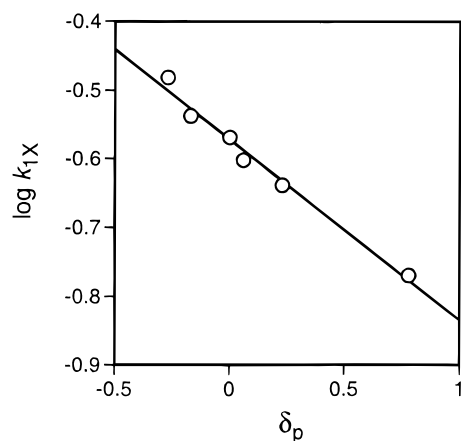


Figure 5. Plot of $\log k_{1X}$ vs δ_p for the iminoquinone formation of **1** with *p*-XC₆H₄CH₂NH₂.

The k_1 value of the amine with an electron-donating *p*-substituent is larger than that of the amine with an electron-withdrawing *p*-substituent. This result is understandable if one considers that the rate-determining step in the iminoquinone formation is the nucleophilic addition of the amine to the quinone (*vide ante*).

At high concentrations of benzylamine (5–25 mM), however, the reaction proceeded to cause the rearrangement of the iminoquinone (**10**) to the product imine (**11**) as seen in the case of benzhydrylamine. Figure 6 shows the spectral change observed upon addition of benzylamine (25 mM) to the CH₃OH solution of **1** (5.0×10^{-5} M) at 30°C under anaerobic conditions. During the course of the reaction, the absorption due to the quinone readily moved to that of iminoquinone **10** (spectrum a), which then decreased with clear isobestic points at 344

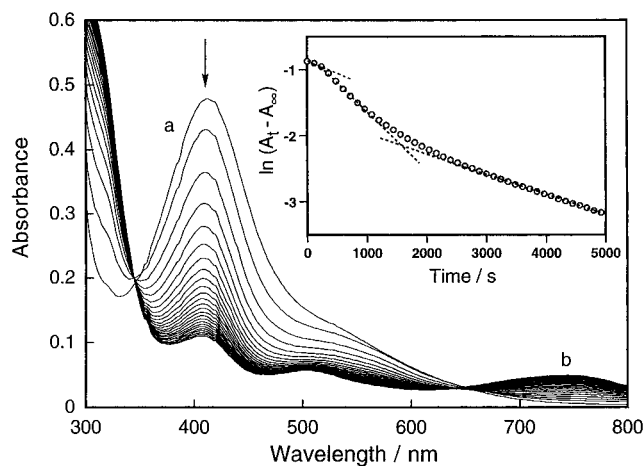


Figure 6. Spectral change observed upon addition of benzylamine (2.5×10^{-2} M) to the methanol solution of **1** (5.0×10^{-5} M) at 30°C under anaerobic conditions; interval, 240 s. Inset: Plot of $\ln(A_t - A_\infty)$ vs time at 420 nm.

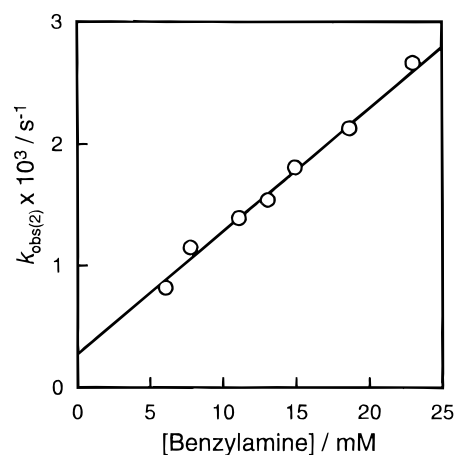


Figure 7. Dependence of k_{obs} on the benzylamine concentration in the reaction of **1** (5.0×10^{-5} M) in methanol at 30°C under anaerobic conditions.

and 660 nm. The absorptions around 400 nm and the shoulder around 520 nm decreased further at the prolonged reaction time, and new absorptions at 507 nm and 755 nm gradually developed (spectrum b in Figure 6). A plot of $\ln(A_t - A_\infty)$ at 420 nm vs time is shown in an inset of Figure 6 where three consecutive steps with three exponential terms are invoked. The first one corresponds to the iminoquinone formation for which the rate constant (k_1) was already determined as shown in Figure 4. The second one may be attributed to the rearrangement of **10** into the product imine **11**, and the third step may correspond to the imine exchange reaction of **11** to produce aminophenol **12**. The observed rate constants, $k_{\text{obs}(2)}$ and $k_{\text{obs}(3)}$, for the second and the third steps were determined by the computer curve fitting with the corresponding exponential terms, respectively. The plot of $k_{\text{obs}(2)}$ vs [amine] gives a straight line with an intercept (Figure 7) as seen in the case of benzhydrylamine (Figure 3B). From the linear plot in Figure 7, the k_2 and k_2' values in eq 1 are determined as $2.4 \times 10^{-4}\text{ s}^{-1}$ and $1.0 \times 10^{-1}\text{ M}^{-1}\text{ s}^{-1}$, respectively. When PhCH₂NH₂ was replaced by PhCD₂NH₂, large deuterium kinetic isotope effects were obtained as 7.8 and 9.2 on both processes, k_2 and k_2' , respectively. Such large kinetic isotope effects confirm that the second step ($k_{\text{obs}(2)}$) corresponds to the product imine formation from the iminoquinone, since

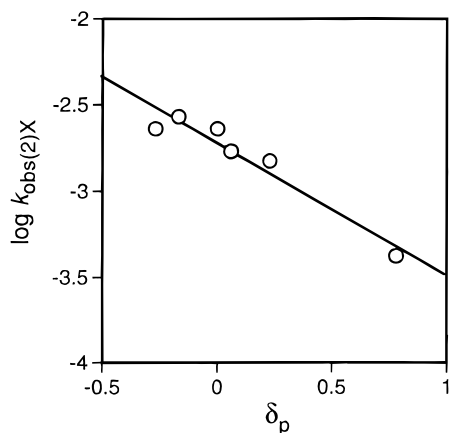


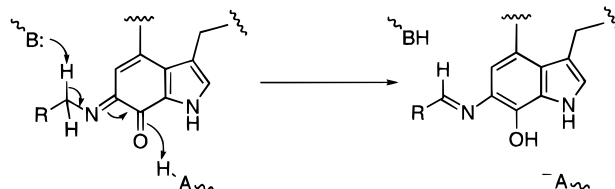
Figure 8. Plot of $\log k_{\text{obs}(2)X}$ vs δ_p for the product imine formation of **1** with $p\text{-XC}_6\text{H}_4\text{CH}_2\text{NH}_2$.

both noncatalyzed (k_2) and general base-catalyzed (k_2') processes involve α -proton abstraction.

In the case of benzhydrylamine (*vide ante*), the k_2 value ($2.9 \times 10^{-4} \text{ s}^{-1}$) is slightly larger than that of benzylamine ($2.4 \times 10^{-4} \text{ s}^{-1}$). In contrast, the k_2' ($8.9 \times 10^{-4} \text{ M}^{-1} \text{ s}^{-1}$) is much smaller than that of benzylamine ($1.0 \times 10^{-1} \text{ M}^{-1} \text{ s}^{-1}$) by 2 orders of magnitude. This seems very reasonable, since the strong conjugation between the C=N bond and the two phenyl rings in the product imine of benzhydrylamine may enhance the spontaneous rearrangement as compared to that in the case of benzylamine. On the other hand, increasing steric hindrance around the amino group will retard the function of general base catalysis, leading to the much smaller k_2' value of benzhydrylamine than that of benzylamine.

The electronic effects of the p -substituents of the benzylamines on the formation of the product imine ($k_{\text{obs}(2)}$) were also examined as shown in Table 3. Plot of the $\log k_{\text{obs}(2)X}$ vs δ_p gave a linear dependence with electron-donating substituents enhancing the rate ($\rho = -0.76$, $r^2 = 0.93$) as shown in Figure 8. The rearrangement process involves α -proton abstraction and the subsequent electron flow from the α -carbon to the quinone moiety to produce product imine. Thus, there may be opposite electronic effects in the two events: one is the α -proton abstraction that favors the electron-withdrawing substituents and the other one is the subsequent electron flow that favors the electron-donating substituents. In the enzymatic reaction there is exhibited a positive correlation between the rate constant of the rearrangement step (II to III in Scheme 1) and δ_p ,^{4b,e} indicating that the electronic effect of the p -substituents enhances the α -proton abstraction in the enzymatic system. On the other hand, the negative effect of the electron-withdrawing substituents was observed in the model system, suggesting that the electron flow from the α -carbon into the quinone moiety is more difficult than in the enzymatic system. Probably, the electron flow from the α -carbon to the quinone moiety may be accelerated by general acid catalysis in the enzyme active site as illustrated in Scheme 4. The crystal structure of the MADH active site suggests that the C-7 carbonyl oxygen is hydrogen-bonded to the

Scheme 4



peptide,² which supports the proposed mechanism illustrated in Scheme 4.

The rate constant k_3 for the formation of aminophenol **12** from **11** was determined as $2.7 \times 10^{-2} \text{ M}^{-1} \text{ s}^{-1}$ from the linear dependence of the observed pseudo-first-order rate constant $k_{\text{obs}(3)}$ on the benzylamine concentration.

Concluding Remarks. The present model studies of TTQ-containing amine dehydrogenases have clearly indicated that the amine oxidation by TTQ cofactor proceeds via a *transamination* mechanism as suggested in the case of the TPQ (TOPA quinone)-catalyzed amine oxidation reaction.^{11,12} The TTQ model compound (**1**) has been shown to be an efficient autorecycling catalyst in the oxidation of benzylamine under aerobic conditions. By employing several amine derivatives, the important reaction intermediates, *substrate imine* and *product imine*, and the reduced product in aminophenol form have been isolated and well characterized by several spectroscopic data. The position of the amine addition to the quinone moiety has been also confirmed to be C-6 by the detailed ¹H NMR analysis. Comparison of the reactivity of **1** in the nonenzymatic system to that of native TTQ in the enzymatic system provides valuable information about the functions of the enzyme itself.

It is interesting to note that all the naturally occurring quinones, TTQ, TPQ, and PQQ, act as an efficient catalyst for the benzylamine oxidation in nonenzymatic systems.^{11b,12b,23a} Although PQQ is now recognized not to be the cofactor of amine oxidases, structural importance for the amine oxidation has been explored by using several PQQ model compounds.^{23,24} Similarly, the importance of the 4-hydroxy-2,5-benzoquinone skeleton of TPQ has been studied extensively in model systems.^{11,12} Thus, examination of the structure-reactivity relationships in the amine oxidation reactions by using several TTQ model compounds (indolequinone derivatives) will provide further insight into the chemical functions of the quinone cofactors.²⁵

Acknowledgment. This work was partially supported by a Grant-in-Aid for Scientific Research on Priority Area (08249223) and for General Scientific Research (08458177) from the Ministry of Education, Science, and Culture, Japan.

JO961705F

(23) (a) Itoh, S.; Mure, M.; Ogino, M.; Ohshiro, Y. *J. Org. Chem.* **1991**, *56*, 6857. (b) Ohshiro, Y.; Itoh, S. *Bioorg. Chem.* **1991**, *19*, 169 and references cited therein.

(24) (a) Sleath, P. R.; Noar, J. B.; Eberlein, G. A.; Bruice, T. C. *J. Am. Chem. Soc.* **1985**, *107*, 3328. (b) Rodriguez, E. J.; Bruice, T. C. *J. Am. Chem. Soc.* **1989**, *111*, 7947.

(25) A portion of the studies was published in: Moenne-Loccoz, P.; Nakamura, N.; Itoh, S.; Fukuzumi, S.; Gorren, A. C. F.; Duine, J. A.; Sanders-Loehr, J. *Biochemistry* **1996**, *35*, 4713.